# Relict blockstreams at Insteheia, Valldalen-Tafjorden, southern Norway: their nature and Schmidt-hammer exposure age.



| | |
|---|---|
| Journal: | *Permafrost and Periglacial Processes* |
| Manuscript ID | PPP-15-0090 |
| Wiley - Manuscript type: | Research Article |
| Date Submitted by the Author: | 30-Oct-2015 |
| Complete List of Authors: | Wilson, Peter; University of Ulster<br>Matthews, John; Swansea University<br>Mourne, Richard; University of the West of England |
| Keywords: | blockstreams, Schmidt-hammer exposure-age dating, Younger Dryas, Norway |

# Relict blockstreams at Insteheia, Valldalen-Tafjorden, southern Norway: their nature and Schmidt-hammer exposure age.

*Peter Wilson[1*], John A. Matthews[2] and Richard W. Mourne[3]*

[1]Environmental Sciences Research Institute, School of Geography and Environmental Sciences, Ulster University, Coleraine, UK

[2]Department of Geography, College of Science, Swansea University, Swansea, UK

[3]Department of Geography and Environmental Management, University of the West of England, Bristol, UK



**Main text: 4,697 words**

*Correspondence to: Peter Wilson, Environmental Sciences Research Institute, School of Geography and Environmental Sciences, Ulster University, Coleraine, Co. Londonderry BT55 1SA, Northern Ireland, UK
E-mail: P.Wilson@ulster.ac.uk

## ABSTRACT

Two small blockstreams, the first such landforms to be recorded in the mountains of Scandinavia, are described from Insteheia, a col at 910 m asl on the watershed between Valldalen and Tafjorden (Møre og Romsdal), southern Norway. Both blockstreams display morphological and sedimentological characteristics indicative of boulder accumulations that have moved downslope by means of solifluction most probably under a permafrost climatic regime. These comprise boulder preferred orientation and dip patterns; inverse grading comprising surface boulders overlying successively finer, well-sorted cobble, pebble and fine-grained (sand/silt dominated) sediment layers; imbrication, with the packing of small boulders behind larger boulders; and proximity to boulder-strewn hillslopes whose constituent boulders (organised into lobes and terraces) feed downslope into the blockstreams. Schmidt-hammer exposure-ages of 7.24 to 11.17 ka indicate that the blockstreams were last active during the Younger Dryas Stadial – Holocene transition (~9.5-11.2 ka). It is inferred that blockstream development began at ~18 ka, following the Last Glacial Maximum, and lasted for ~8 ka, and that since the blockstreams became inactive fine-grained material has been progressively lost as a result of snowmelt runoff. The small areal extent and relatively recent age of the blockstreams contrast with larger-scale forms of considerably greater age in the Southern Hemisphere.


KEY WORDS: blockstreams, Schmidt-hammer exposure-age dating, Younger Dryas, Norway

## INTRODUCTION

Accumulations of coarse rock debris are common components of the landform assemblage in many areas of past and present periglacial conditions (Ballantyne and Harris, 1994; French, 2007). Depending on the local topographic context, primarily slope gradient and elevation, and the severity of climate, such debris accumulations may assume different morphological expression. Thus, blockfields, blockslopes, blockstreams, boulder lobes, debris flows, talus, rock avalanches and rock glaciers are frequently distinguished. However, because these forms can occur in close proximity and often grade into one another, it can be difficult to isolate and delimit them. Furthermore in certain locations the age and origin of some of these features have proved to be contentious (Rea, 2013). Establishing the mechanics and timing of their formation is important with respect to developing integrated models of Quaternary landscape evolution and change.

Blockstreams, also termed rock streams, stone runs and kurums, are one manifestation of coarse debris accretion by mass-wasting processes (Wilson, 2013). They are linear deposits that extend a greater distance downslope than across slope and vary in topographic setting from open hillslopes to valley axes. Most reports of blockstreams concern relict features (e.g. Boelhouwers *et al*., 2002; Caine and Jennings, 1968; Clark, 1972; Firpo *et al*., 2006; Gutiérrez and Gutiérrez, 2014; Nelson *et al*., 2007; Potter and Moss, 1968; Smith, 1953), and indicate that variations in plan form, dimensions, morphology, structure and composition exist. Plan configurations range from straight or sinuous single-thread forms to dendritic, braided or anastomosing styles. They range from a few tens of metres in width and a few hundred metres in length to several hundred metres in width and up to 5 km in length. Generally, openwork rock debris is common to all blockstreams but their surfaces may be diversified by randomly distributed pits and elongated depressions, and/or extensive longitudinal furrows. Moreover prominent surface steps, ridges and lobes may be present.

Blockstream development is favoured by well-jointed igneous and metamorphic rocks because their widely-spaced joints predispose them to macrogelivation, thermal stress fracturing, and/or deep chemical weathering, resulting in the production of many large blocks. Many examples have been recorded on basalt, dolerite and quartzite. Stratigraphically blockstreams display inverse grading and a lack of interstitial fine-grained material in at least their uppermost part. In some locations blockstreams extend downslope from summit and plateau blockfields as a result of debris transport; in others they originate from hillslope scarps or tor-like outcrops. Active blockstreams are apparently less frequent than relict occurrences and there are correspondingly fewer detailed accounts: Harris *et al*. (1998) being a rare instance.

Several attempts have been made to establish the age of relict blockstreams. Caine and Jennings (1968) obtained a $^{14}C$ age of 35.2+1.6/-2.15 ka from wood beneath blockstream debris in southeastern Australia and from this attributed blockstream formation to a subsequent cold stage, corresponding with the (global) Last Glacial Maximum (LGM; ~27-19 ka). Samples of basal soil and peat covering Tasmanian blockfields have yielded $^{14}C$ ages of 4.7-3.08 ka, indicating blockfield (and by inference blockstream) stability throughout at least the late Holocene; additionally, weathering rind thickness measurements of blockfield clasts suggests stability has persisted for the past ~13 ka (Caine, 1983). Cosmogenic isotope ($^{36}Cl$) surface exposure dating applied to blockstreams and blockslopes in southeastern Australia has given a cluster of ages within the limits of the LGM, with a weighted mean exposure age of 21.9±0.5 ka (Barrows *et al*., 2004). However, two boulders returned ages of 498 ka and 157 ka, demonstrating that some blockstream elements are considerably older than the LGM. Application of cosmogenic isotope ($^{10}Be$ and $^{26}Al$) surface exposure dating to blockstreams in the Falkland Islands produced ages ranging from 731 ka to 42 ka, indicating development of these features spanned at least 690 ka, that their activity likely extends over several cold stages, and that they are long-lived, composite landforms (Wilson *et al*., 2008). In contrast to these results Hansom *et al*. (2008) reported optically stimulated luminescence ages ranging from >54 ka to 16 ka on samples of fine-grained material beneath Falkland Islands blockstreams. These ages suggest some Falkland blockstreams were active during the LGM.

Although relict blockstreams have been identified in many areas that experienced severe periglacial conditions, they do not appear to have been recorded as such in Scandinavia. This may be because of the extent of glacier ice cover during the LGM; examples from elsewhere are in locations that were beyond the limits of LGM ice. However, this is unlikely to account for their apparent absence because numerous reports exist of blockfields on Scandinavian mountains, especially from Norway (Fjellanger *et al*., 2006; Follestad, 1990; Juliussen and Humlum, 2007; Kleman and Borgström, 1990; Nesje, 1989; Rea *et al*., 1996; Sellier, 1995; Whalley *et al*., 1997, 2004). Given the close morphological and topographical association between some blockfields and blockstreams it would seem that the latter probably do exist in parts of Scandinavia and were likewise buried beneath LGM ice. Their apparent absence from the literature may be because they have been subsumed under the term blockfields.

This paper focuses on a small area of coarse rock debris at Insteheia, southern Norway, the disposition and nature of which are considered diagnostic of relict blockstreams. Specific aims are: (1) to describe the morphological and sedimentological characteristics of the first explicit example of blockstreams from Scandinavia; (2) to apply Schmidt-hammer exposure-age dating (SHD) to blockstreams for the first time; and (3) to discuss the implications of our findings for theories of blockstream development and processes of formation.

## RESEARCH AREA

Insteheia (910 m asl; Grid Reference MQ 159094) is a broad col aligned southwest– northeast on the watershed between Valldalen and Tafjorden (Møre og Romsdal), southern Norway (Figures 1 and 2). Slopes to the north of the col rise to Mefjellet (1100 m asl), those to the south rise to Hegguraksla (1219 m asl). The latter are longer and steeper than those to the north but both slopes are boulder-strewn with boulders organised into lobes and terraces. North-facing slopes are also diversified by low degraded bedrock scarps and are cliffed, in parts, above ~1150 m asl.

The bedrock geology of the site is migmatic gneiss (Tveten *et al*., 1998). During the LGM the col lay well below the altitudinal limit of the continental ice sheet. Although there has been considerable debate about ice thicknesses and extent of ice-free terrain in this northwestern part of southern Norway at the LGM (e.g. Brook *et al*., 1996; Follestad, 1990; Nesje *et al*., 1987; Winguth *et al*., 2005), the altitudinal limit of the ice sheet appears to have lain at 1400-1500 m (Goehring *et al*, 2008). However, the col was not inundated by glacier ice during the Younger Dryas Stadial (YDS; 12.9-11.7 ka) which, in this area, is evidenced by valley glacier moraines in Valldalen to the north and end moraines of two small cirque glaciers to the east beneath Blåfjellet (Carlson *et al*., 1983). At present Insteheia is within the alpine zone but below the lower limit of contemporary permafrost (Etzelmüller *et al*., 2003; Lilleøren *et al*., 2012). Climatic data for AD 1961-90 for Tafjord meteorological station (15 m asl), 9 km south-southeast of Insteheia, reveal a mean annual air temperature (MAAT) of 6.9 °C and mean annual precipitation (MAP) of 965 mm (Aune, 1993; Førland, 1993). Using a lapse rate of 0.65 °C per 100 m (Lilleøren *et al*., 2012) the MAAT at Insteheia reduces to 1.1 °C with mean monthly temperatures below 0 °C for six months of the year (Table 1). MAP at Insteheia cannot be estimated with accuracy but it is likely to be considerably higher than at Tafjord; in addition, more than half of the MAP is likely to fall as snow at Insteheia given the estimated negative temperature values for six months of the year.

The floor of the col and the slopes falling southwest towards Tafjorden and northeast towards Valldalen are covered by coarse rock debris disposed in the form of blockstreams. The boulder-strewn lower hillslopes north and south of the col merge downslope with the blockstreams, suggesting these slopes were the source ('feeders') of the debris. For clarity, we term the blockstream descending southwest from the col blockstream A and that to the northeast blockstream B.

## FIELD METHODS AND RATIONALE

Long axis gradients of the blockstreams and some of the feeder accumulations on the lower hillslopes were determined with an Abney level. At each of four locations 30 boulders were measured for their long (*a*) axis orientation and dip of their *a-b* plane. These locations were 'paired', with each pair comprising a blockstream sample and an associated sample from the adjacent feeder-area. At a single location on each blockstream shallow (~0.6 m deep) pits were hand-excavated to examine the vertical structure of the boulder accumulations. Fine-grained material (<2 mm) sampled from a depth of ~0.5-0.6 m in each pit was subjected to particle size analysis using a Malvern Mastersizer, following organic matter digestion and dispersion in a weak solution of sodium hexametaphosphate (Calgon). Schmidt-hammer R-values were measured on surface boulders using two mechanical 'N-type' Schmidt hammers (Proceq, 2006) the reliability of which were checked before and after use with the manufacturer's test anvil (McCarroll, 1987, 1994; Winkler and Matthews, 2014). Mean R-values were derived from single blows on each of 100 boulders at eight locations; four of the locations were those used for boulder orientation and dip measurements. The other four were from another location on blockstream A; from the highest part of the col (the blockstream divide); and from another location on blockstream B and its associated feeder area. All locations are indicated on Figure 2. Boulder surfaces selected for SHD measurements were horizontal or near-horizontal, and corners, cracks, lichen thalli and wet areas were avoided (Matthews and Wilson, 2015).

Schmidt-hammer R-values derived from boulder-rich landforms are an indicator of the time elapsed since exposure of rock surfaces of uniform lithology to subaerial weathering and, in the case of blockstreams, the timing of boulder stabilisation. The technique has developed as one of high-precision calibrated dating for which statistical confidence intervals can be generated (Matthews and Owen, 2010; Matthews and Winkler, 2011; Matthews and McEwan, 2013; Matthews and Wilson, 2015). At least two surfaces of known age (young and old control points), lithologically equivalent to the rock surface being dated, are required for calibration.

For the present paper we used two young and three old control surfaces, which are described in Matthews and Wilson (2015). The first young control is from the boulders of a rockfall that occurred about 10 years ago at 900 m asl on the north side of Langfjelldalen, 19 km northeast of Insteheia; the second is from bedrock outcrops in a series of road cuts, with average age of ~20 years, between the village of Fjøra, on Tafjorden, and the mountain farm of Nysætra at 750 m asl (Figure 1). The three old control surfaces are boulders on YDS moraines (Carlson *et al*., 1983). The first is at 850-900 m asl in Alnesdalen, 23 km northeast of Insteheia; the other two are at 950-1050 m asl in Trollkyrkjebotn to the north of Blåfjellet (Figure 1). These sites have been assigned an age of 11.5 ka in accordance with the very late occurrence of the YDS ice-sheet maximum in western Norway (Bondevik and Mangerud, 2002), and also allowing for a short phase of moraine stabilisation and glacier retreat following the YDS termination at 11.7 ka in the Greenland ice core chronology (Rasmussen *et al*., 2006; Walker *et al*., 2009; Carlson, 2013). The lithology of the Trollkyrkjebotn sites is augengneiss rather than the migmatic gneiss of the other sites (Tveten *et al*., 1998), which may have an influence on the R-values from these control points. However, any effect is considered to be minor because R-values from the other control site of the same age (Alnesdalen) are not significantly different.

## SCHMIDT-HAMMER EXPOSURE AGE CALIBRATION AND AGE ESTIMATION

Age-calibration is described for this area by Matthews and Wilson (2015), following the procedures developed by Matthews and Owen (2010), Matthews and Winkler (2011), Matthews and McEwen (2013) and Matthews *et al*. (2014). The high-precision calibration equation was based on combined data for both of the young control surfaces and combined data for the three old control surfaces (Table 2). Thus the linear calibration equation was based on two control points of known age (Matthews and Owen, 2010; Shakesby *et al*., 2011) and each control point utilised all the data available from the control surfaces. This is justified by the generally consistent mean R-values found from control surfaces of known age in the area (Matthews and Wilson, 2015).

The equations used for age calibration, including the calculation of 95% confidence intervals around predicted SHD ages, are as follows (see also Matthews *et al*., 2014; Matthews and Wilson, 2015). The calibration equation is a standard linear regression equation of the form:

$$y = a + bx$$

where $x$ is mean R-value and $y$ is surface age in years. For two control points, the $b$ coefficient (slope of the calibration curve) is defined by:

$$b = (y_1 - y_2)/(x_1 - x_2)$$

where $x_1$ and $x_2$ are the mean R-values of the older and younger control points, respectively, and $y_1$ and $y_2$ are their respective ages. The $a$ coefficient (intercept age) is obtained by substitution in the calibration equation.

The 95% confidence interval for age, which represents the total error ($C_t$), combines the error of the calibration curve at the point associated with the sample surface being dated ($C_c$) with the sampling error residing in the sample itself ($C_s$):

$$C_t = \sqrt{(C_c^2 + C_s^2)}$$



The error of the calibration curve is calculated from the errors associated with the control points and their difference in age:

$$C_c = C_o - [(C_o - C_y)(R_s - R_o)/(R_y - R_o)]$$

where $C_o$ is the 95% confidence interval of the old control point in years, $C_y$ is the confidence interval of the young control point in years, and $R_o$, $R_y$ and $R_s$ are the mean R-values of the old control point, the young control point and the sample surface, respectively. The sampling error associated with the sample surface depends on the slope of the calibration curve ($b$), the sample size ($n$), Student's $t$ statistic and the standard deviation ($s$) of the R-values from the sample surface:

$$C_s = b[ts/\sqrt{(n-1)}]$$

## RESULTS

### Blockstream dimensions and morphology

Exposed boulders occupy ~0.2 km$^2$ of the Insteheia col in several areas of irregular plan form (Figure 2). An additional ~0.35 km$^2$ of adjacent ground is covered by thin (<0.3 m) vegetated peat from which boulders project and in which gaps reveal underlying boulders, demonstrating that the extent of boulders is substantially greater than indicated by the surface exposures alone. Blockstream description and measurement were restricted to the areas of exposed boulders.

Blockstream A extends southwest from the col for ~0.8 km along the valley axis as a generally narrow (~15-250 m wide) zone of open-work boulders with a single-thread to braided plan form (Figures 3a, b). The downvalley terminus is a prominent topographic step extending over a distance of 10 m at a gradient of 12º. Water issues from the base of the step and continues downslope in an open fluvial channel constrained by vegetated banks. Above the step, blockstream gradients are reduced to within the range 0-5º with no marked breaks of slope and boulder *b* axes are generally between 0.15 m and 1.5 m. In several places water flow was either seen or heard at shallow depth (<0.5 m) between boulders, and vegetation debris draped across and around some boulders indicates recent surface water flow. At a distance of ~0.6 km up-valley from its terminus the blockstream gradient is 0º over a distance of 60 m and numerous small (<1 m wide) pools of shallow (<0.2 m deep) standing water were present when these sites were visited in early August. Many of the boulders in this area are covered by moss.

The continuity of blockstream A is disrupted as the col is approached by a more extensive cover of vegetated peat; exposed boulders form several distinct ‘islands’ (Figure 3c) and adjacent boulder-strewn ‘feeder’ slopes rise at gradients of up to 12º.

Blockstream B extends northeast from the col for ~0.2 km as a broad swathe of boulders that is substantially shorter (downslope) but wider (across-slope) than A. The maximum boulder *b* axis is 2.5 m with several boulders in the range 1.5-2.5 m (Figure 3d).

The terminus of blockstream B is less pronounced than that of A, with a gradual transition from boulders to vegetated ground extending over ~20-30 m. No water was seen or heard beneath blockstream B although persistent fluvial flow begins a short distance downslope of the terminus. This may indicate a greater thickness of boulders is present in B but there are no exposures to support this inference, or to show the nature of blockstream substrate.

Throughout all areas of the blockstreams the *a-b* planes of the majority of boulders appear to dip upslope (Figure 3e), whilst boulders exposed in the predominantly vegetated areas define shallow (<50 cm deep) linear troughs or pits and have no apparent preferred orientation or dip (Figure 3f). These troughs and pits are suggestive of depressed margins associated with large-scale sorted patterned ground, and this is supported by the slightly elevated adjacent ground. In addition, there are a few large boulders upslope of which smaller boulders are jammed because their onward movement has been effectively prevented.

**Boulder orientation and dip**

Boulder orientation and dip data for pairs of samples (1 and 3, 7 and 8) from blockstream and feeder-area boulders are presented in Figure 2. For all samples the majority of *a* axis orientations fall within ±45º of the slope aspect; most boulders are therefore aligned parallel or sub-parallel to local slope aspect. Some transverse or sub-transverse boulder alignments are evident in each sample, most prominently in feeder-area samples 3 and 8 with 40% and 13% of their boulders respectively.

Up-slope dipping boulders are dominant (73-86%) at each site. Most boulders dip at <30º but generally greatly exceed local ground surface gradient. Maximum boulder dip is 48º.

**Blockstream structure and particle size**

The hand-excavated pits show similar arrangements of inversely graded coarse debris (Figure 4). Below the cover of surface boulders there are successively finer, well-sorted cobble, pebble and sand /silt-rich sediment layers. The fine-grained materials encountered at the base of the pits yielded 43% sand, 45% silt and 12% clay at E1, and 80% sand, 17% silt and 3% clay at E2. Cumulative frequency curves for each sample plotted against the frost-susceptibility limit of Beskow (1935) are shown in Figure 5. For the most part both samples plot within the frost susceptible zone.

**Schmidt-hammer R-value measurements and SHD ages**

Schmidt-hammer R-values for the control sites are summarised in Table 2 and combined frequency distributions for the two young sites and the three old sites are shown in Figure 6. These data indicate an R-value difference of 17.5 units between recently exposed rock surfaces (~15 years; mean R-value 56.39) and surfaces dating from 11.5 ka (mean R-value 38.89). Two of the three old control surfaces, Alnsedalen moraine and Trollkyrkebotn moraine (west), have indistinguishable mean R-values, whereas the mean R-value from Trollkyrkebotn moraine (east) differs from these at the 95% level; however, given that they do not differ at the 99% level it is considered appropriate to combine all three sites into a single control point. Using these data the high-precision calibration equation and curve shown in Figure 7 were derived.

Frequency distributions of R-values from blockstream samples (Figure 8) are generally similar (despite high variability of values; range 18-67) in being near-symmetrical and either uni- or multi-modal. In these respect they mirror the combined frequency distribution for the old control sites and may be interpreted as indicating a single population of boulders. The SHD exposure age of each blockstream sample, based on mean R-values (Table 3), was determined from the calibration equation of $y = 37022.951 – 656.28571x$ given in Figure 6. These ages and their 95% confidence intervals ($C_t$), together with the error components used to estimate the confidence intervals – i.e. the sampling error associated with each blockstream sample ($C_s$) and the error in the calibration curve ($C_c$) – are listed in Table 4. Ages range from 7.24 ka to 11.17 ka – a span of ~4 ka. As most of the 95% confidence intervals overlap, the ages cannot be regarded as statistically different from one another at the 5% significance level.

Whilst the age of site 2 (7.24 ka) does not differ statistically from the second youngest site (8: 9.5 ka) it does differ from all the other sites; possible reasons for this are explored below. The average age of the samples is 9.96 ka, but if site 2 is excluded from the calculation the average age is 10.35 ka. Irrespective of the difference and the reliability of the site 2 age, exposure of the boulders dates from the YDS – Holocene transition.

## DISCUSSION

### Blockstream origin

In contrast to relict blockstreams recorded from other areas of the world (e.g. Caine, 1983; Boelhouwers *et al*., 2002; Wilson *et al*., 2008) the blockstreams at Insteheia occupy rather small land surface areas and may be regarded as immature examples of the landform. Nevertheless they display characteristics that are commensurate with more extensive cases, namely: (1) patterns in preferred boulder orientation and dip that are usually regarded as indicative of downslope movement; (2) inverse grading of debris with surface boulders overlying well-sorted cobble, pebble, and fine-grained sediment layers that are frost susceptible; (3) imbricate smaller boulders packed behind larger boulders indicating their downslope movement has been impeded; and (4) a close spatial association with large-scale sorted patterned ground and boulder-strewn hillslopes on which boulders are organised into lobes and terraces, and which merge downslope as they feed into the blockstreams. The inference is that blockstream development is the result of former periglacial hillslope processes.

Moreover, alternative origins for the blockstreams, in particular fluvial and/or glacial processes, would be difficult to substantiate. Boulder emplacement by fluvial action can be rejected because adjacent hillslopes provide very little by way of catchment area to generate sufficient high-magnitude runoff capable of moving boulders of the noted dimensions. Furthermore, the hillslopes lack networks of incised fluvial channels suggesting that they have been and continue to be characterised by patterns of diffuse surface and/or subsurface flow. Glacial processes can also be rejected as a possible explanation for boulder accumulation. Although Insteheia was covered by ice during the LGM, blockstream morphology does not conform to known styles of glacial deposition. Similarly, the movement of boulders downslope from the col to both southwest and northeast cannot be reconciled with ice movement across this area.

The mechanics of blockstream movement have been discussed on several previous occasions (see Wilson (2013) for a recent review) and several processes working in combination or succession have been proposed, but the apparent absence of currently active forms of similar scale to relict examples has restricted understanding. It has frequently been proposed that boulders must have moved downslope in association with a matrix of fine-grained sediment by the process of solifluction (with or without the presence of permafrost); frost heave and creep have been regarded as subsidiary processes. The absence of fine-grained material in the upper thicknesses of blockstreams has led to the assumption that after blockstream movement ceased the flow of surface or sub-surface water removed the matrix. Although this may have happened, it raises the issue of how distinct patterns of boulder orientation and dip originate. If such patterns develop during blockstream movement then the removal of matrix would likely cause some rearrangement of boulders as they settle.

Therefore boulder orientations and dips may represent, at least in part, settlement fabrics rather than transport fabrics. At present, at Insteheia and other relict blockstreams, the former presence and nature of interstitial fine-grained material is not known with certainty and thus the mechanics of downslope movement cannot be satisfactorily resolved.

**Blockstream age**

The SHD ages indicate that the surficial boulders of the blockstreams became inactive in the transition from the YDS to the Holocene. Because there are no significant differences in SHD ages between the 'axial' blockstream sites and the 'feeder' areas it can be inferred that the whole system was probably active and then became relict at approximately the same time. We infer that blockstream development is likely to have begun in a permafrost environment following the retreat of LGM ice at ~18 ka BP with frost-wedged boulders from hillside outcrops and local glacially-plucked boulders, in association with fine-grained material, being solifluncted downslope. Blockstream activity is also likely to have continued through the YDS: if there had been limited or no activity in the YDS older SHD ages would be expected.

The relatively young age from site 2 is from the area of blockstream A where the gradient is 0º and there are numerous small pools of standing water. This younger age (7.24±1.2 ka) is not incompatible with some blockstream activity during brief early-Holocene cooling events, such as those at 9.7-10.2 ka (the Erdalen Event in Norway) and at 8.2 ka (the Finse Event in Norway) when mountain glaciers underwent expansion (Dahl *et al*., 2002; Nesje *et al*., 2008) and periglacial activity was likely enhanced. This may have resulted in the annual freeze-thaw regime being more effective at moving boulders in the presence of a higher ground-water table.

Although the SHD ages indicate that most blockstream activity ceased at the transition from the YDS to the Holocene, the present status of the blockstreams was likely attained after they had experienced a lengthy period of non-permafrost conditions early in the Holocene. During this period, fine-grained material is likely to have been removed from their uppermost parts under a periglacial environment characterised by a cool temperate climatic regime with seasonally frozen ground, particularly as a consequence of snowmelt runoff from adjacent slopes.

The apparent absence of blockstreams elsewhere in Scandinavia may be because previous workers have not discriminated them from blockfields. But in areas that are currently underlain by permafrost and dominated by coarse rock debris with extensive areas of sorted circles and sorted stripes (e.g. the Juvvasshytta area of Jotunheimen, southern Norway, at 1850 m asl; Ødegård *et al*., 1987, 1988) blockstream absence may be due to the lack of a period of non-permafrost conditions during which the removal of fines could occur to give blockstreams their characteristic morphology.

## CONCLUSIONS

Two relict blockstreams, the first to be recognised in the mountains of Scandinavia, have been identified at Insteheia, a col at 910 m asl between Valldalen and Tafjorden, southern Norway. Although of small areal extent the blockstreams display morphological characteristics commensurate with more extensive examples described from other regions of the world. The blockstreams are devoid of fine-grained material in their upper thicknesses but are characterised by a well-sorted vertical structure with overall inverse grading and basal fine-grained material, display patterns of boulder orientation and dip that indicate downslope movement has occurred, exhibit boulder imbrication with clusters of smaller boulders packed behind larger boulders suggesting some impedance of movement has occurred, and pass upslope into boulder-strewn hillslopes with lobate and terrace morphology. Whereas these characteristics are consistent with formation by periglacial processes, there remain several unanswered questions in relation to blockstream formation. The site demonstrates that blockstream-forming processes have operated since the LGM, that similar features should be present elsewhere in the Norwegian mountains, and that such sites have general implications for understanding slope evolution under periglacial climatic conditions.

If, as inferred, the blockstreams began developing after the LGM and became inactive, as indicated by SHD, during the YDS – Holocene transition, their downslope movement spanned a period of ~8 ka. The small areal extents of the Insteheia blockstreams are therefore entirely consistent with a short period of formation. This relatively short interval contrasts markedly with the considerably longer timespans (~5-7 ka x $10^2$) recorded for blockstream development in Southern Hemisphere locations (at some of these sites blockstreams extend 1-5 km downslope). Our results suggest, therefore, that blockstream development can take place relatively rapidly if suitable environmental conditions pertain and, consequently, that the much older ages obtained from relict blockstreams elsewhere may merely indicate very long periods of inactivity combined with the propensity of boulder landforms to persist in the landscape.

**ACKNOWLEDGEMENTS**

Fieldwork was conducted on the Swansea University Jotunheimen Research Expeditions, 2014 and 2015. The line diagrams were prepared by Kilian McDaid at Ulster University. This paper constitutes Jotunheimen Research Expeditions, Contribution No. xxx.

## REFERENCES


Aune B. 1993. Temperaturnormaler: Normalperiode 1961-90. Det Norske Meteorologiske Institutt: Oslo.

Ballantyne CK, Harris C. 1994. *The periglaciation of Great Britain*. Cambridge University Press, Cambridge.

Barrows TT, Stone JO, Fifield LK. 2004. Exposure ages for Pleistocene periglacial deposits in Australia. *Quaternary Science Reviews* **23**: 697-708.

Beskow G. 1935. Soil freezing and frost heaving with special applications to roads and railroads. In Historical perspectives in frost heave research: the early works of S. Taber and G. Beskow, Black PB, Hardenburg MJ (eds). US Army Corps of Engineers, Special Report 91-23, 1991.

Boelhouwers JC, Holness S, Meiklejohn I, Sumner P. 2002. Observations on a blockstream in the vicinity of Sani Pass, Lesotho Highlands, Southern Africa. *Permafrost and Periglacial Processes* **13**: 251-257.

Bondevik S, Mangerud, J. 2002. A calendar age estimate of a very late Younger Dryas ice sheet maximum in western Norway. *Quaternary Science Reviews* **21**: 1661-1676.

Brook EJ, Nesje A, Lehman SJ, Raisbeck GM, Yiou F. 1996. Cosmogenic nuclide exposure ages along a vertical transect in western Norway: implications for the height of the Fennoscandian ice sheet. *Geology* **24**: 207-210.

Caine N. 1983. The Mountains of Northeastern Tasmania. Balkema, Rotterdam, The Netherlands.

Caine N, Jennings JN. 1968. Some blockstreams of the Toolong Range Kosciusko State Park, New South Wales. *Journal and Proceedings, Royal Society of New South Wales* **101**: 93-103.

Carlson AB, Sollid JL, Torp B. 1983. *Valldal Kvartaergeologi og geomorphologi, 1319 IV [Valldal Quaternary Geology and Geomorphology, Sheet 1319 IV] 1:50,000.* Geografisk Institutt, Universitetet i Oslo, Oslo.

Carlson AE. 2013. The Younger Dryas climate event. In Encyclopedia of Quaternary Science, Elias SA (ed.). Elsevier, Amsterdam; **3**: 126-134.

Clark R. 1972. Periglacial landforms and landscapes in the Falkland Islands. *Biuletyn Peryglacjalny* **21**: 33-50.

Dahl SO, Nesje A, Lie Ø, Fjordheim K and Matthews JA. 2002. Timing, equilibrium-line altitudes and climatic implications of two early-Holocene glacier readvances during the Erdalen Event at Jostedalsbreen, southern Norway. *The Holocene* **12**: 17-25.

Etzelmüller B, Berthling I. Sollid JL. 2003. Aspects and concepts on the geomorphological significance of Holocene permafrost in southern Norway. *Geomorphology* **52**: 87-104.

Firpo M, Guglielmin M, Queirolo C. 2006. Relict blockfields in the Ligurian Alps (Mount Beigua, Italy). *Permafrost and Periglacial Processes* **17**: 71-78.

Fjellanger J, Sørbel L, Linge H, Brook EJ, Raisbeck GM, Yiou F. 2006. Glacial survival of blockfields on the Varanger Peninsula, northern Norway. *Geomorphology* **82**: 255-272.

Follestad BA. 1990. Block fields, ice flow directions and the Pleistocene ice sheet in Nordmøre and Romsdal, west Norway. *Norsk Geologisk Tidsskrift* **70**: 27-33.

Førland EJ. 1993. Nedbørnormaler: Normalperiode 1961-90. Det Norske Meteorologiske Institutt: Oslo.

French HM. 2007. *The periglacial environment*. 3rd edition. Wiley, Chichester.

Goehring BM, Brook EJ, Linge H, Raisbeck GM, Yiou F. 2008. Beryllium-10 exposure ages of erratic boulders in southern Norway and implications for the history of the Fennoscandian Ice Sheet. *Quaternary Science Reviews* **27**: 320-336.

Gutiérrez M, Gutiérrez F. 2014. Block streams in the Tremendal massif, central Iberian Chain. In Landscapes and Landforms of Spain, Gutiérrez F, Gutiérrez M (eds). Springer, Dordrecht; 187-195.

Hansom JD, Evans DJA, Sanderson DCW, Bingham RG, Bentley MJ. 2008. Constraining the age and formation of stone runs in the Falkland Islands using Optically Stimulated Luminescence. *Geomorphology* **94**: 117-130.

Harris SA, Cheng G, Zhao X, Yongqin D. 1998. Nature and dynamics of an active block stream, Kunlun Pass, Qinghai Province, People's Republic of China. *Geografiska Annaler* **80A**: 123-133.

Juliussen H, Humlum O. 2007. Preservation of block fields beneath Pleistocene ice sheets on Sølen and Elgåhogna, central-eastern Norway. *Zeitschrift für Geomorphologie* **51**: 113-138.

Kleman J, Borgstrøm I. 1990. The boulder fields of Mt. Fulufjället, west-central Sweden. *Geografiska Annaler* **72A**: 63-78.

Lilleøren KS, Etzelmüller B, Schuler TV, Gisnås K, Humlum O. 2012. The relative age of mountain permafrost – estimation of Holocene permafrost limits in Norway. *Global and Planetary Change* **92-93**: 209-223.

Matthews JA, McEwen LJ. 2013. High-precision Schmidt-hammer exposure-age dating (SHD) of flood berms, Vetlestølsdalen, alpine southern Norway: first application and some methodological issues. *Geografiska Annaler* **95A**: 185-194.

Matthews JA, Owen 2010. Schmidt-hammer exposure-age dating: developing linear age-calibration curves using Holocene bedrock surfaces from the Jotunheimen-Jostedalsbreen regions of southern Norway. *Boreas* **39**: 105-115.

Matthews JA, Winkler S. 2011. Schmidt-hammer exposure-age dating (SHD): application to early Holocene moraines and a reappraisal of the reliability of terrestrial cosmogenic-nuclide dating (TCND) at Austanbotnbreen, Jotunheimen, Norway. *Boreas* **40**: 256-270.

Matthews JA, Wilson P. 2015. Improved Schmidt-hammer exposure ages for active and relict pronival ramparts in southern Norway, and their palaeoenvironmental implications. *Geomorphology* **246**: 7-21.

Matthews JA, Winkler S, Wilson P. 2014. Age and origin of ice-cored moraines in Jotunheimen and Breheimen, southern Norway: insights from Schmidt-hammer exposure-age dating. *Geografiska Annaler* **96A**: 531-548.

McCarroll D. 1987. The Schmidt hammer in geomorphology: five sources of instrument error. *British Geomorphological Research Group, Technical Bulletin* **36**: 16-27.

McCarrroll D. 1994. The Schmidt hammer as a measure of the degree of rock surface weathering and terrain age. In Dating in Exposed and Surface Contexts, Beck C (ed.). University of New Mexico Press, Albuquerque, 29-46.

Nelson KJP, Nelson FE, Walegur MT. 2007. Periglacial Appalachia: palaeoclimatic significance of blockfield elevation gradients, eastern USA. *Permafrost and Periglacial Processes* **18**: 61-73.

Nesje A. 1989. The geographical and altitudinal distribution of block fields in southern Norway and its significance to the Pleistocene ice sheets. *Zeitschrift für Geomorphologie* Supplement-Band **72**: 41-53.

Nesje A, Anda E, Rye N, Lien R, Hole PA, Blikra LH. 1987. The vertical extent of the late Weichselian ice sheet in the Nordfjord-Møre area, western Norway. *Norsk Geologisk Tidsskrift* **67**: 125-141.

Nesje A, Bakke J, Dahl SO, Lie Ø, Matthews JA. 2008. Norwegian mountain glaciers in the past, present and future. *Global and Planetary Change* **60**: 10-27.

Ødgård R, Liestøl O, Sollid JL. 1987. Juvflya Kvartærgeologi og Geomorphologi, 1:10,000. Geografisk Institutt, Universitetet-i-Oslo.

Ødgård R, Liestøl O, Sollid JL. 1988. Periglacial forms related to terrain parameters in Jotunheimen, southern Norway. *Proceedings 5th International Permafrost Conference, Trondheim* **3**: 59-61.

Potter N, Moss JH. 1968. Origin of the Blue Rocks block field and adjacent deposits, Berks County, Pennsylvania. *Geological Society of America Bulletin* **79**: 255-262.

Proceq. 2006. *Operating instructions (Betonprüfhammer N/NR-L/LR).* Proceq SA, Schwerzenbach.

Rasmussen SO, Andersen KK, Svensson AM, Steffensen JP, Vinther BM, Clausen HB, Siggaard-Andersem M.-L, Johnsen, SJ, Larsen LB, Dahl-Jensen D, Bigler M, Röthlisberger

R, Fischer H, Goto-Azuma K, Hansson ME, Ruth U. 2006. A new Greenland ice core chronology for the last glacial termination. *Journal of Geophysical Research* **111**: D06102.

Rea BR. 2013. Blockfields (Felsenmeer). In Encyclopedia of Quaternary Science, Elias SA (ed.). Elsevier, Amsterdam; **3**: 523-534.

Rea BR, Whalley WB, Rainey MM, Gordon JE. 1996. Blockfields old or new? Evidence and implications from some plateaus in northern Norway. *Geomorphology* **15**: 109-121.

Sellier D. 1995. Le felsenmeer du Mont Gausta (Telemark, Norvège): environnement, caractères morphologiques et significations paléogéographiques. *Géographie physique et Quaternaire* **49**: 185-205.

Shakesby RA, Matthews JA, Karlen W, Los S. 2011. The Schmidt hammer as a Holocene calibrated-age dating technique: testing the form of the R-value – age relationship and defining predicted errors. *The Holocene* **21**: 615-628.

Smith HTU. 1953. The Hickory Run boulder field, Carbon County, Pennsylvania. *American Journal of Science* **251**: 625-642.

Tveten E, Lutro O, Thorsnes T. 1998. *Geologisk kart over Norge, berggrunskart Ålesund* [*Geological map of Norway: bedrock map, Ålesund sheet*] *1:250,000*. Norges Geologiske Undersøkelse. Trondheim.

Walker MJC, Johnsen S, Rasmussen SO, Popp T, Steffensen J-P, Gibbard P, Hoek W, Lowe J, Andrews J, Björck S, Cwynar LC, Hughen K, Kershaw P, Kromer B, Litt T, Lowe DJ, Nakagawa T, Newnham R, Schwander J. 2009. Formal definition and dating of the GSSP (Global Stratotype Section and Point) for the base of the Holocene using the Greenland NGRIP ice core, and selected auxiliary records. *Journal of Quaternary Science* **24**: 3-17.

Whalley WB, Rea BR, Rainey MM, McAlister J. 1997. Rock weathering in blockfields: some preliminary data from mountain plateaus in north Norway. In Palaeosurfaces: recognition, reconstruction and palaeoenvironmental interpretation, Widdowson M (ed.). Geological Society Special Publication **120**: 133-145.

Whalley WB; Rea BR, Rainey MM. 2004. Weathering, blockfields, and fracture systems and the implications for long-term landscape formation: some evidence from Lyngen and Øksfordjøkelen areas in north Norway. *Polar Geography* **28**: 93-119.

Wilson P. 2013. Block/rock streams. In Encyclopedia of Quaternary Science, Elias SA (ed.). Elsevier, Amsterdam; **3**: 514-522.

Wilson P, Bentley MJ, Schnabel C, Clark R, Xu S. 2008. Stone run (block stream) formation in the Falkland Islands over several cold stages, deduced from cosmogenic isotope ($^{10}$Be and $^{26}$Al) surface exposure dating. *Journal of Quaternary Science* **23**: 461-473.

Winguth C, Mickleson DM, Larsen E, Darter JR, Moeller CA, Stalsberg K. 2005. Thickness evolution of the Scandinavian Ice Sheet during the late Weichselian in Nordfjord, western Norway: evidence from ice-flow modelling. *Boreas* **34**: 176-185.

Winkler S, Matthews JA. 2014. Comparison of electronic and mechanical Schmidt hammers in the context of exposure-age dating: are Q- and R-values interconvertible? *Earth Surface Processes and Landforms* **19**: 1128-1136.

**Figure captions:**

**Figure 1.** Location of Insteheia, Valldalen-Tafjorden. 1. Area of blockstreams (see Figure 2 for detail), 2. Younger Dryas moraines of the Trollkyrkjebotn cirques, 3. Streams and water bodies, 4. Contours in metres. Scale is given by 1 km marginal grid.

**Figure 2.** Plan of the Insteheia blockstreams showing locations of excavated pits (E1 and E2), SHD sites (1-8), and plots of *a* axis orientations (full rose) and *a-b* plane dips (half rose) for four of the SHD sites. Class intervals are 20º for orientation data and 10º for dip data.

**Figure 3. a**: Up-valley view of blockstream A showing a single-thread plan form immediately above its terminal step. The survey pole is 1 m long. **b**: Up-valley view of blockstream A displaying a braided plan form at approximately mid-way between its terminus and the col. **c**: The discontinuous nature of exposed boulders in the col; view is from south to north. **d**: Down-valley view of part of blockstream B. The person (JAM) is standing beside the largest boulder (*b* axis of 2.5 m). **e**: Upslope-dipping boulders at site 1 on blockstream A; the survey pole is 1 m long. **f**: Boulders outline a curvi-linear depression in a predominantly vegetated area adjacent to blockstream A. The survey pole is 1 m long.

**Figure 4. a:** Undisturbed blockstream surface at site of excavation E1. **b:** Well-sorted angular and sub-angular cobbles directly below the boulders shown in photo **a**. **c:** Water-table below the cobbles in photo **b**. **d:** Angular and sub-angular cobbles directly below surface boulders in excavation E2. In each photo the scale bar divisions are 6 cm. Locations of E1 and E2 are indicated in Figure 2. **e:** Sketch based on blockstream structure in E1 and E2 showing inverse grading of debris and water table position.

**Figure 5.** Cumulative frequency curves for the two samples of fine-grained material from the excavated pits plotted against the frost-susceptibility limit of Beskow (1935).

**Figure 6.** Combined frequency distributions of Schmidt-hammer R-values for the two young control sites (N = 750) and three old control sites (N = 1125). Class interval is 2 units.

**Figure 7.** High-precision calibration equation and curve based on Schmidt-hammer data for young and old control sites.

**Figure 8.** Frequency distributions of Schmidt-hammer R-values for the blockstream sites. N = 100 for each site; class interval is 2 units.

**Tables:**

**Table 1.** Mean monthly and annual air temperatures and precipitation for Tafjord meteorological station (15 m asl) AD 1961-90, and estimated mean monthly and annual temperatures for Insteheia (910 m asl).

**Table 2.** Schmidt-hammer R-values from the control sites: data used for the calibration equation are shown in bold.

**Table 3.** Schmidt-hammer R-values from the blockstream samples.

**Table 4.** Schmidt-hammer exposure-ages (SHD) for the blockstream samples. Each SHD age has a 95% confidence interval ($C_t$) derived from the sampling error of the blockstream sample ($C_s$) and the error associated with the calibration curve ($C_c$).

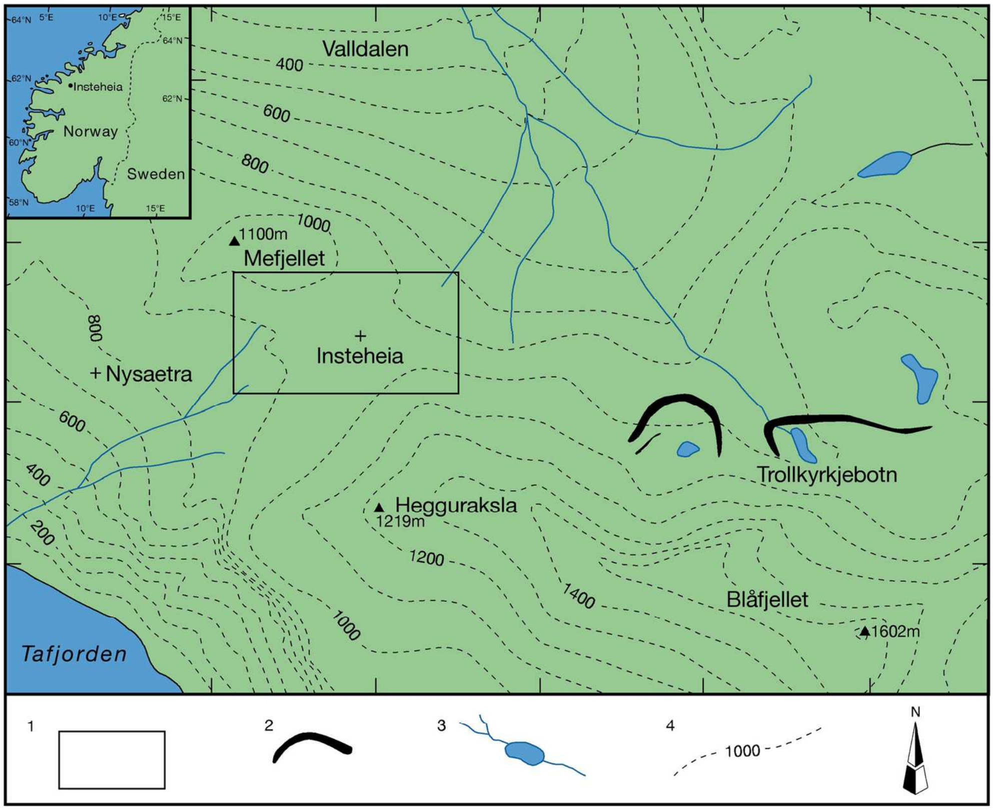


Figure 1
150x126mm (300 x 300 DPI)

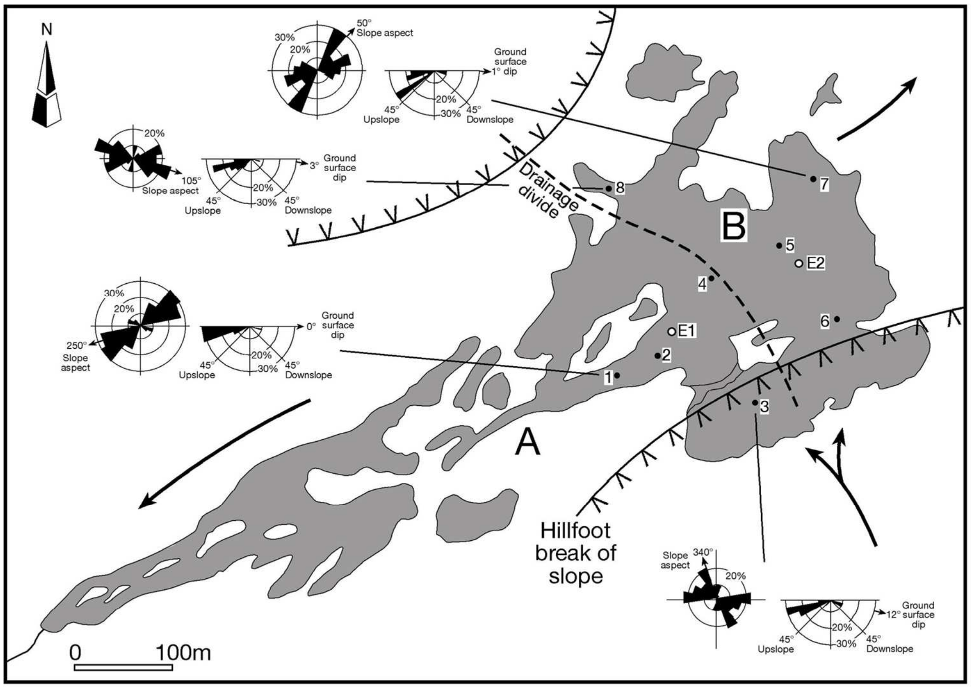


Figure 2
150x109mm (300 x 300 DPI)

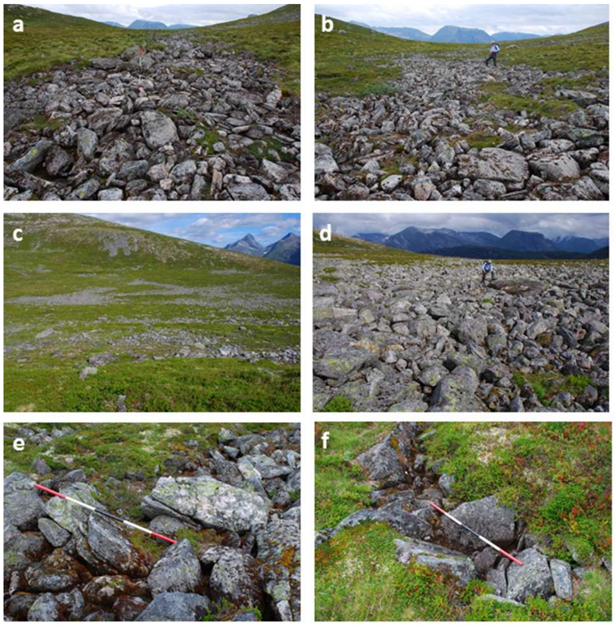


Figure 3
285x190mm (96 x 96 DPI)

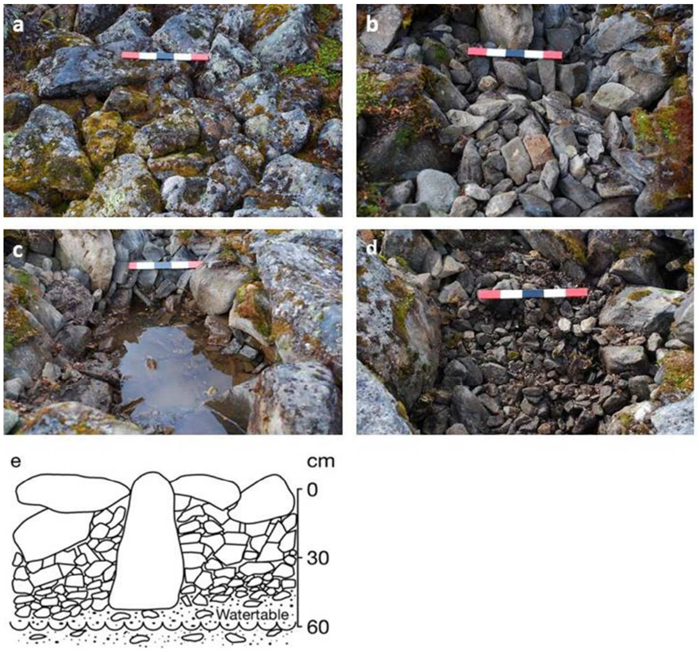


Figure 4
285x190mm (96 x 96 DPI)

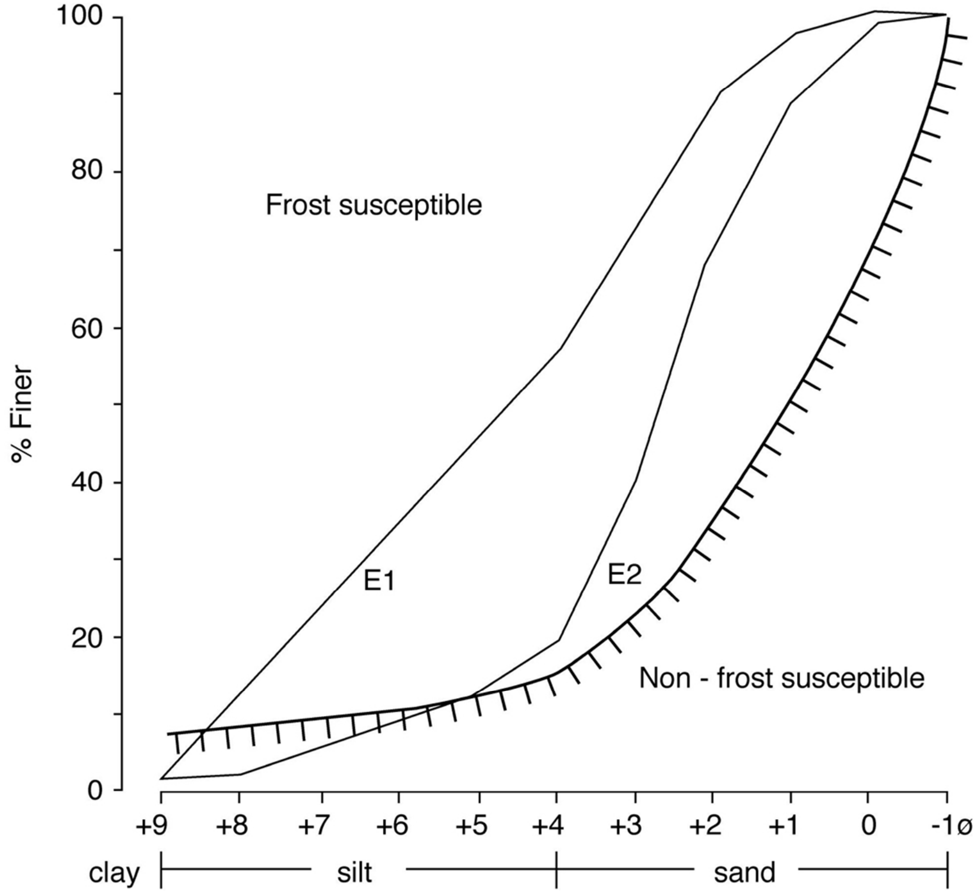


Figure 5
99x90mm (300 x 300 DPI)

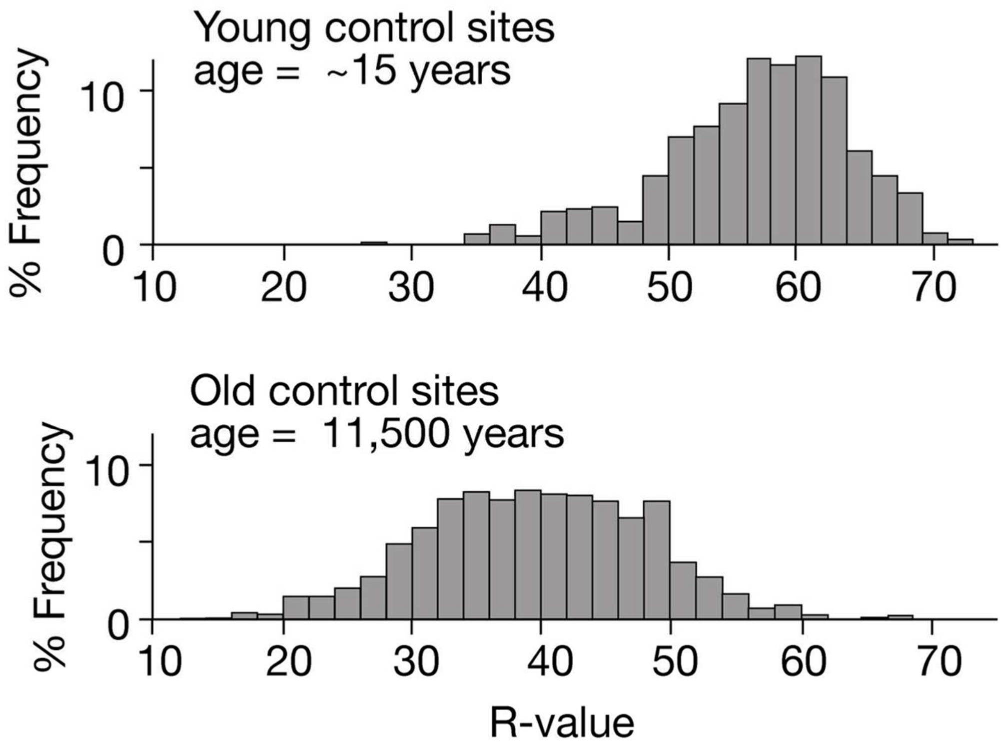


Figure 6
99x74mm (300 x 300 DPI)

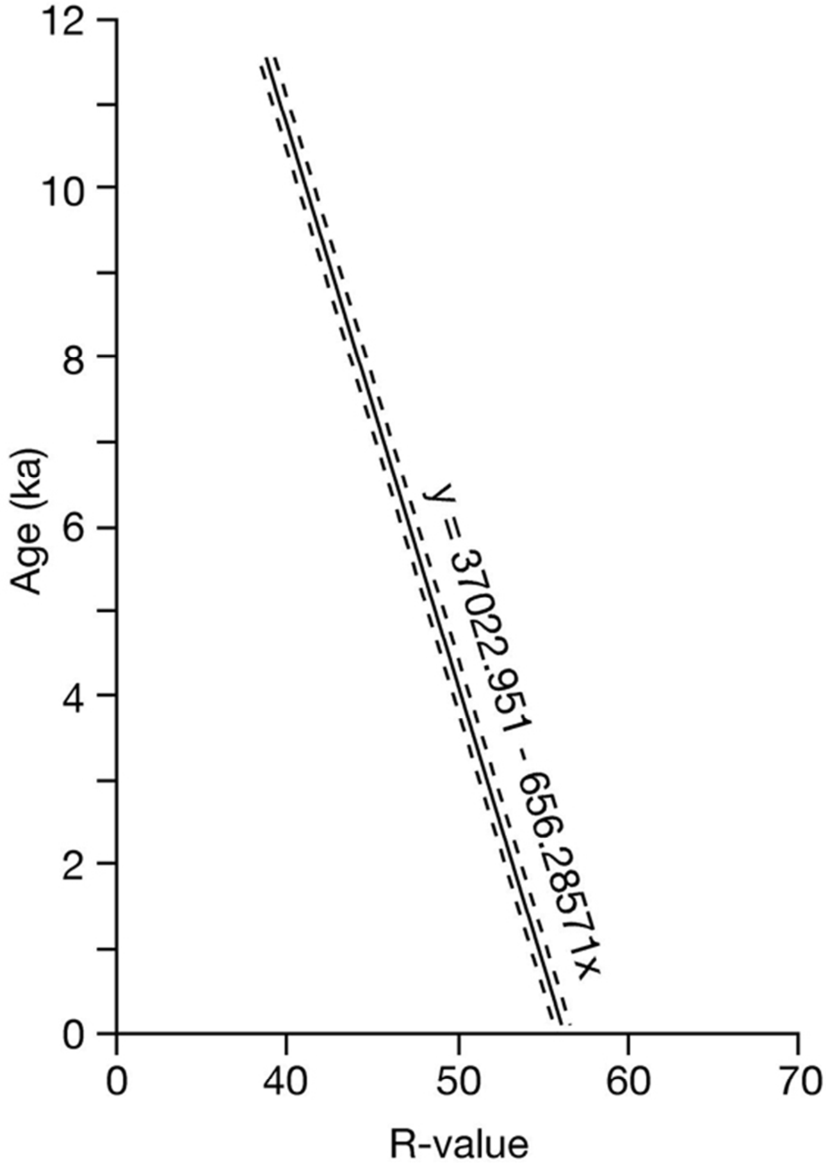


Figure 7
50x69mm (300 x 300 DPI)

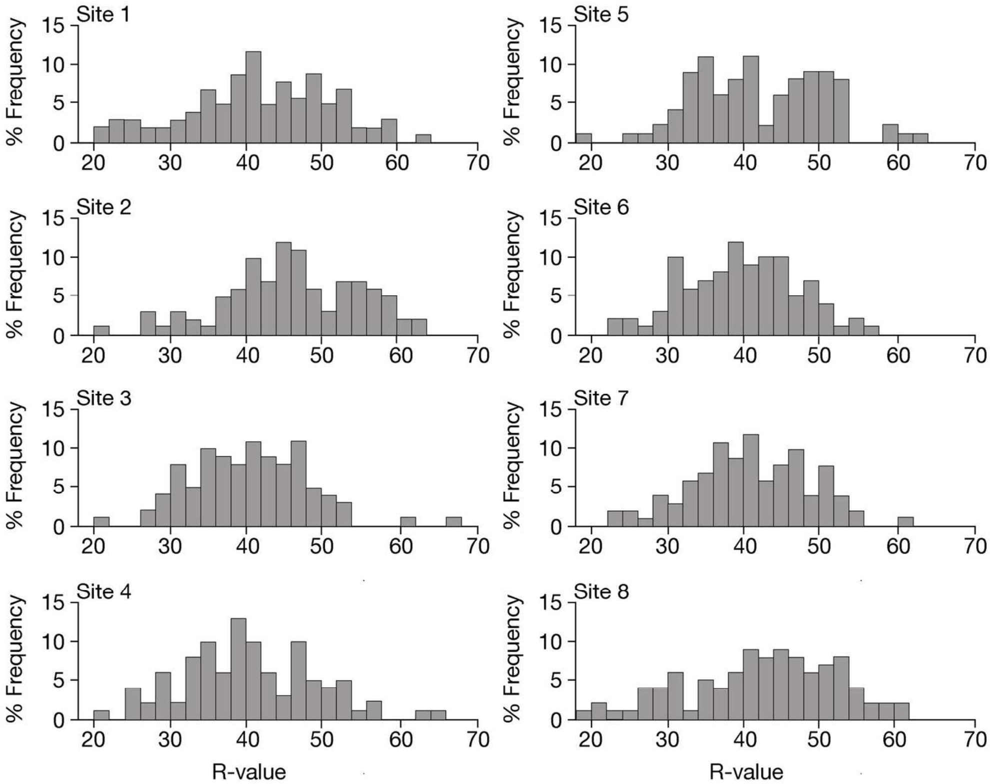


Figure 8
150x117mm (300 x 300 DPI)

Table 1. Mean monthly and annual air temperatures and precipitation for Tafjord meteorological station (15 m asl) AD 1961-90, and estimated mean monthly and annual temperatures for Insteheia (910 m asl).

| | Jan | Feb | Mar | Apr | May | Jun | Jul | Aug | Sep | Oct | Nov | Dec | Annual |
|---|---|---|---|---|---|---|---|---|---|---|---|---|---|
| *Air temperature (°C)* | | | | | | | | | | | | | |
| Tafjord | 0.5 | 0.7 | 2.7 | 5.2 | 10.1 | 12.7 | 13.9 | 13.7 | 10.5 | 8 | 3.6 | 1.3 | 6.9 |
| Inesteheia | -5.3 | -5.1 | -3.1 | -0.6 | 4.3 | 6.9 | 8.1 | 7.9 | 4.7 | 2.2 | -2.2 | -4.5 | 1.1 |
| *Precipitation (mm)* | | | | | | | | | | | | | |
| Tafjord | 100 | 76 | 82 | 53 | 35 | 41 | 60 | 64 | 101 | 107 | 115 | 131 | 965 |

Table 2. Schmidt-hammer R-values from the control sites: data used for the calibration equation are shown in bold.

| Control Point | Age (years) | Mean R-value | Standard deviation | Confidence interval (95%) | N |
|---|---|---|---|---|---|
| *Young sites* | | | | | |
| Langfjelldalen rockfall | 10 | 55.59 | 7.61 | 0.77 | 375 |
| Fjøra road cuttings | 20 | 57.18 | 7.02 | 0.71 | 375 |
| Young sites combined | **15** | **56.39** | **7.32** | **0.53** | **750** |
| *Old sites* | | | | | |
| Alnesdalen moraine | 11,500 | 39.64 | 9.69 | 0.99 | 375 |
| Trollkyrkebotn moraine (west) | 11,500 | 39.58 | 7.6 | 0.77 | 375 |
| Trollkyrkebotn moraine (east) | 11,500 | 37.44 | 8.46 | 0.86 | 375 |
| Old site combined | **11,500** | **38.89** | **8.62** | **0.5** | **1125** |

Table 3. Schmidt-hammer R-values from the blockstream samples.

| Sample | Mean R-value | Standard deviation | Confidence interval (95%) | N |
|---|---|---|---|---|
| 1 | 41.36 | 9.3739 | 1.87 | 100 |
| 2 | 45.38 | 8.836 | 1.76 | 100 |
| 3 | 39.98 | 7.5749 | 1.51 | 100 |
| 4 | 39.87 | 8.6633 | 1.73 | 100 |
| 5 | 41.44 | 8.398 | 1.67 | 100 |
| 6 | 39.4 | 7.4301 | 1.48 | 100 |
| 7 | 40.48 | 7.6818 | 1.53 | 100 |
| 8 | 41.94 | 9.7825 | 1.95 | 100 |

Table 4. Schmidt-hammer exposure-ages (SHD) for the blockstream samples. Each SHD age has a 95% confidence interval ($C_t$) derived from the sampling error of the blockstream sample ($C_s$) and the error associated with the calibration curve ($C_c$) .

| Sample | SHD age (years) | $C_t$ - 95% confidence interval (years) | $C_s$ (years) | $C_c$ (years) |
|---|---|---|---|---|
| 1 | 9880 | ±1270 | 1227 | 331 |
| 2 | 7240 | ±1205 | 1156 | 335 |
| 3 | 10,785 | ±1045 | 991 | 329 |
| 4 | 10,855 | ±1180 | 1134 | 329 |
| 5 | 9825 | ±1150 | 1099 | 331 |
| 6 | 11,165 | ±1030 | 974 | 329 |
| 7 | 10,455 | ±1060 | 1005 | 330 |
| 8 | 9500 | ±1320 | 1280 | 332 |